The Consequences of Chromosomal Aneuploidy on Gene Expression Profiles in a Cell Line Model for Prostate Carcinogenesis

John L. Phillips,[1] Simon W. Hayward, Yuzhuo Wang, James Vasselli, Christian Pavlovich, Hesed Padilla-Nash, John R. Pezullo, B. Michael Ghadimi, Gary D. Grossfeld, Alexandra Rivera, W. Marston Linehan, Gerald R. Cunha, and Thomas Ried

Urologic Oncology Branch [J. L. P., J. V., C. P., W. M. L.], Genetics Branch [H. P-N., B. M. G., T. R.], Laboratory of Pathology [A. R.], Center for Cancer Research, National Cancer Institute, NIH, Bethesda, Maryland 20817; Department of Pharmacology, Georgetown University School of Medicine, Washington, DC 20007 [J. R. P.]; and Departments of Urology [S. W. H., G. D. G., G. R. C.] and Anatomy [Y. W., G. R. C.], University of California-San Francisco, San Francisco, California 94143

ABSTRACT

Here we report the genetic characterization of immortalized prostate epithelial cells before and after conversion to tumorigenicity using molecular cytogenetics and microarray technology. We were particularly interested to analyze the consequences of acquired chromosomal aneuploidies with respect to modifications of gene expression profiles. Compared with nontumorigenic but immortalized prostate epithelium, prostate tumor cell lines showed high levels of chromosomal rearrangements that led to gains of 1p, 5, 11q, 12p, 16q, and 20q and losses of 1pter, 11p, 17, 20p, 21, 22, and Y. Of 5700 unique targets on a 6.5K cDNA microarray, ~3% were subject to modification in expression levels; these included *GRO-1, -2, IAP-1,- 2, MMP-9*, and *cyclin D1*, which showed increased expression, and *TRAIL*, *BRCA1*, and *CTNNA*, which showed decreased expression. Thirty % of expression changes occurred in regions the genomic copy number of which remained balanced. Of the remainder, 42% of down-regulated and 51% of up-regulated genes mapped to regions present in decreased or increased genomic copy numbers, respectively. A relative gain or loss of a chromosome or chromosomal arm usually resulted in a statistically significant increase or decrease, respectively, in the average expression level of all of the genes on the chromosome. However, of these genes, very few (*e.g.*, 5 of 101 genes on chromosome 11q), and in some instances only two genes (*MMP-9* and *PROCR* on chromosome 20q), were overexpressed by ≥1.7-fold when scored individually. Cluster analysis by gene function suggests that prostate tumorigenesis in these cell line models involves alterations in gene expression that may favor invasion, prevent apoptosis, and promote growth.

INTRODUCTION

The characterization of genetic events at early stages of prostate carcinogenesis has been limited by the paucity of suitable cell line models. This difficulty is a reflection of the often slow-growing nature of most prostate cancers *in vivo*. Studies using loss of heterozygosity analyses, CGH,[2] and fluorescent *in situ* hybridization revealed few recurrent chromosomal aberrations in early prostate cancers (1–3). Such analyses point to a remarkable genetic heterogeneity in prostate cancer, even between lesions from different regions of the same prostate gland (4–5). Generally, however, low-stage primary tumors tend to be near diploid with few clonal numerical and/or structural aberrations, which include gains of chromosome 7 and losses of 8p and 10q (6–7). In contrast, high-stage, advanced primary or metastatic prostate tumors tend to be aneuploid, have a high degree of chromosomal aberrations and, in general, are typified more by chromosomal loss than by DNA amplification (2, 8). Normal prostate epithelium,

hyperplastic lesions, and cells from primary tumors have been immortalized and viral oncogenes have been used to establish cell lines reflective of low-grade and early-stage disease.

A large T-antigen immortalized human prostatic epithelial cell line, BPH-1, was derived from nonneoplastic benign prostate hyperplasia (9). BPH-1 does not form tumors in nude mice but will remain viable for up to 12 months after transplantation. By G-banding, BPH-1 is near triploid, contains an isochromosome 3q, a deletion of 8p, translocations involving chromosomes 10 and 15, and six unidentified marker chromosomes (9). BPH-1 becomes tumorigenic after *in vivo* coculture with CAFs (Fig. 1; Ref. 10). Resulting TD cell lines (BPH1^CAFTD) remain tumorigenic after retransplantation without CAFs. BPH-1 also undergoes malignant transformation after tissue recombination with rUGM in TE-treated host mice resulting in the TD cell lines BPH1^TETD-A and -B (11). The phenotypic and cellular changes during conversion to tumorigenicity are described in the accompanying article by Hayward *et al.* (12). Here we report a comprehensive analysis of genetic aberrations that correlate with the acquisition of tumorigenicity. We were especially interested to establish how acquired chromosomal aneuploidies, a common feature of malignant tumors, modify the expression levels of genes residing on the affected chromosomes. We have therefore used SKY and CGH to complement cDNA microarray analysis to characterize chromosomal changes and to assess the consequences of aneuploidy on gene expression levels.

MATERIALS AND METHODS

Cells. BPH-1, BPH1^CAFTD-01, -02, -03, -04, and BPH1^TETD-A and -B were grown in a 5% CO_2 humidified atmosphere in RPMI (Clonetics, Rockville, MD) supplemented with 10% fetal bovine serum (Life Technologies, Inc., Grand Island, New York), epithelial growth factor (5 ng/ml), insulin (1 µg/ml), and transferrin (5 µg/ml; Ref. 12).

Molecular Cytogenetics. Metaphase chromosomes were obtained as described previously (13). SKY kits were hybridized to metaphase chromosomes as reported previously (14). Images were acquired with SkyView software (Applied Spectral Imaging, Ltd., Migdal Haemek, Israel) using a spectral cube and a charge-coupled device camera (Hamamatsu, Bridgewater, NJ) connected to a DMRXA microscope (Leica, Wetzlar, Germany) with a custom-designed SKY-3 optical filter (Chroma Technology, Brattleboro, VT). DNA was prepared using high-salt extraction methods. For CGH, biotin-labeled tumor DNA and digoxigenin-labeled normal donor DNA (sex-matched) was cohybridized to sex-matched normal human lymphocyte metaphase chromosomes and detected, and images were acquired and analyzed with Q-CGH (Leica Imaging Systems, Cambridge, United Kingdom) software (15).

Microarrays. cDNA microarray analysis was performed in quintuplicate on BPH-1 and BPH1^CAFTD-01 using the NCI Oncochip.[3] Briefly, 40 µg of total sample (BPH-1 or "tumor" BPH1^CAFTD-01) cell line RNA and 50 µg of "pooled" reference total RNA were labeled using reverse transcriptase to incorporate CY3-dUTP and CY5-dUTP (Amersham, Piscataway, NJ), respectively. We prepared reference RNA by pooling equal amounts of total cell line RNA from cervical (HeLa), lung (H157), and breast (MCF-7) carcinoma,
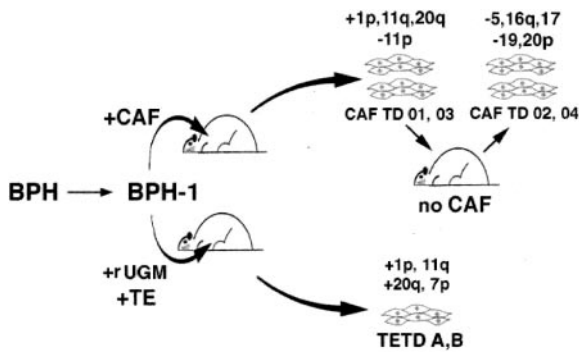
Fig. 1. Derivation of tumor strains and accompanying chromosomal aberrations. Noncancerous human prostate epithelial cells (*BPH*) were immortalized with large T antigen (Tag) to create the cell line BPH-1, as described in detail in the accompanying article by Hayward *et al.* (12). BPH-1 undergoes transformation into the first generation tumors BPH^{CAFTD}-01 and -03 and acquires gains of 1p, 11q, 20q and relative loss of 11p compared with BPH-1. BPH^{CAFT}-01 and -03 become the second generation tumors BPH^{CAFTD}-02 and -04, respectively, without CAF acquiring losses of 5, 16q, 17, 19, and 20p. Alternatively, BPH-1 forms tumors in TE-stimulated mice resulting in tumors (BPH^{TETD}-A, -B) and acquire gains of 1p, 7p, 11q, and 20q.

embryonic kidney 293, and K562 pluripotent hematopoietic stem cell. Probe preparation, array hybridization, and imaging were described previously (16, 17). The ratio $\{\Sigma[\text{tumor/pool}]/n_1\}:\{[\Sigma(\text{BPH-1/pool})]/n_2\}$ where n_1 and n_2 = the number of evaluable arrays ≥ 3 for each sample, was used to algebraically remove pool target values and to allow comparison of BPH-1 *versus* tumor (BPH1^{CAFTD}-01). Evaluable genes printed in duplicate or more were excluded from analysis if the ratios were discordant. We considered thresholds for down- and up-regulation of genes as tumor:BPH-1 ratios of <0.50 and >1.50, respectively. We also considered genes with ratios of 0.50–0.75 as down-regulated if derived from data representing ≥ 9 slides. We used a *U* test[4] to assess for the statistical significance between the paired, nonparametric microarray datasets. For genes that reached threshold criteria in all five of the array pairs but had no band assignment, we "BLAST-mapped" them by searching the Human Genome resources with GenBank sequences.[5] We assigned a band to the "mined" gene of interest when flanking contigs or other genes had concordant band assignments.

Zymography. Zymography was used to assess for MMP-9 and MMP-2 proteolytic activity after electrophoretic separation under nonreducing conditions. Briefly, conditioned medium was obtained from 2-h serum-deprived cells at 70–80% confluency. A total of 4.5 μg protein for each sample was electrophoresed in a 10% zymogram gel (Invitrogen, Carlsbad, CA) containing MMP substrate, and was incubated for 18 h in zymography buffer (18). The degree of digestion, as assessed by the density of the bands after electrophoresis and incubation, is directly proportional to enzyme activity.

RESULTS

Molecular Cytogenetics. SKY and CGH of CAFs, BPH-1, and the tumorigenic derivatives of BPH-1 was performed to establish a baseline of chromosomal copy number alterations for the interpretation of gene expression changes.

SKY of BPH-1 revealed a near triploid cell line with 14 clonal and 33 nonclonal unbalanced translocations and refined previous G-banding analysis (Ref. 9; Table 1).[6] Numerical chromosomal aberrations detected by SKY included the loss of chromosome 4 and gains of chromosomes 14, 15, 17, 20, and X.

By SKY, all tumor-derived cell lines shared the near-triploidy, isochromosome 3q, and unbalanced translocations involving 8p, 9p, and 10p seen in BPH-1.[7] All of the tumors share a duplication of

---

[4] Internet address for *U* test: www.statibot.com. Other statistical software used can be found at member.aol.com/johnp71/javastat.html.

[5] Internet address: www.ncbi.nlm.nih.gov.

[6] Full results are at http://www.ncbi.nlm.nih.gov/sky/skyweb.cgi and in the ISCN table in "Appendix."

[7] Full results are at http://www.ncbi.nlm.nih.gov/sky/skyweb.cgi.

bands 1p13→1p33 and loss of 1p34→pter. Karyotypically, the transition from CAF-derived (tumors -01 and -03) to the "second generation," CAF-independent (tumors -02 and -04) involves continued rearrangement of harlequin chromosomes involving 7p, 11q, and 20, and chromosomal loss of 5, 16, 17, 18, and 19. No additional chromosomal gains or losses were seen. The TE BPH tumor derivatives (BPH1^{TETD}-A and -B) shared many cytogenetic abnormalities of the BPH1^{CAFTD} tumors. The few observed differences can be retrieved from the karyotype[6] and include the presence of nonreciprocal and reciprocal translocations.

The large degree of chromosomal instability and the high number of chromosomal translocations in BPH-1 and the tumorigenic cell lines that were derived from BPH-1 prompted us to complement the SKY results using CGH. CGH analysis of BPH-1, BPH1^{CAFTD}, and BPH1^{TETD} showed that the cell lines share certain features including loss of chromosome 4 and gains of X and 14, loss of 8p and 10p attributable to multiple unbalanced translocations, and loss of 3p and gain of 3q as predicted from the presence of an isochromosome 3q (see www.ncbi.nlm.nih.gov/sky/skyweb.cgi for profiles). On this background, multiple differences arise during tumorigenic conversion of BPH-1. First, new 3p derivatives (markers 16 and 28) clonally emerge in the first generation of CAF-derived but not TE-derived tumors. In addition, a chromosome 3 fragment is replicated within harlequin chromosomes. Thus, in the first generation of CAF-derived tumors, the 3p loss appears limited to 3p11→3p21. Gains of 1p13→p33 and loss from 1p34→pter in all generations of CAF- and TE-derived tumors reflect the 1p duplication seen by SKY (Fig. 2, *A* and *B*).

The genomic replication of the (11;20)(q;q) fragment as seen by SKY in the tumorigenic lines resulted in a 2- to 4-fold gain of 11q13→11q22 and 20q12→18 in CAF- and TE-derived lines (Fig. 2, *C* and *D*). The 20q amplification appeared similar in the tumor lines, regardless of the mode of induction, and comprised essentially the entire long arm. Additional differences between BPH-1 and the first generation tumors were the relative loss of 1p34→36, 8p22→ter, 9q22→24, 11p13→14, 15, 17, 20p, 21, 22, and Y and gains of 5, 6p, 7q11.2→7p14, 7p21→pter, 12p, 14, 16q, and X (Fig. 3). All of the chromosomal aberrations in the first generation tumors were main-

Table 1 *Recurrent selected markers in BPH-1 and representative tumor cell lines*

Shown is transition (⇒) from parental line, BPH-1, to first generation line (BPH-^{CAFTD}-01), which becomes the second generation line (BPH^{CAFTD}-02). On right is TETD line derived from BPH-1. Markers are described in ISCN karyotype table in the "Appendix."[a]

	BPH-1 (parental)⇒	BPH^{CAFTD}-01⇒	BPH^{CAFTD}-02	(BPH-1)⇒BPH^{TETD}-A
M1	+	+	+	+
M3	+	+	+	+
M8	+	+	+	+
M14	+	+	+	
M15		+	+	+
M16		+	+	
M18		+	+	
M19		+		
M20		+	+	+
M21		+	+	+
M22		+		+
M23			+	
M26			+	
M27			+	
M38				+
M39				+
M41				+
M42				+
M43				+
M44				+

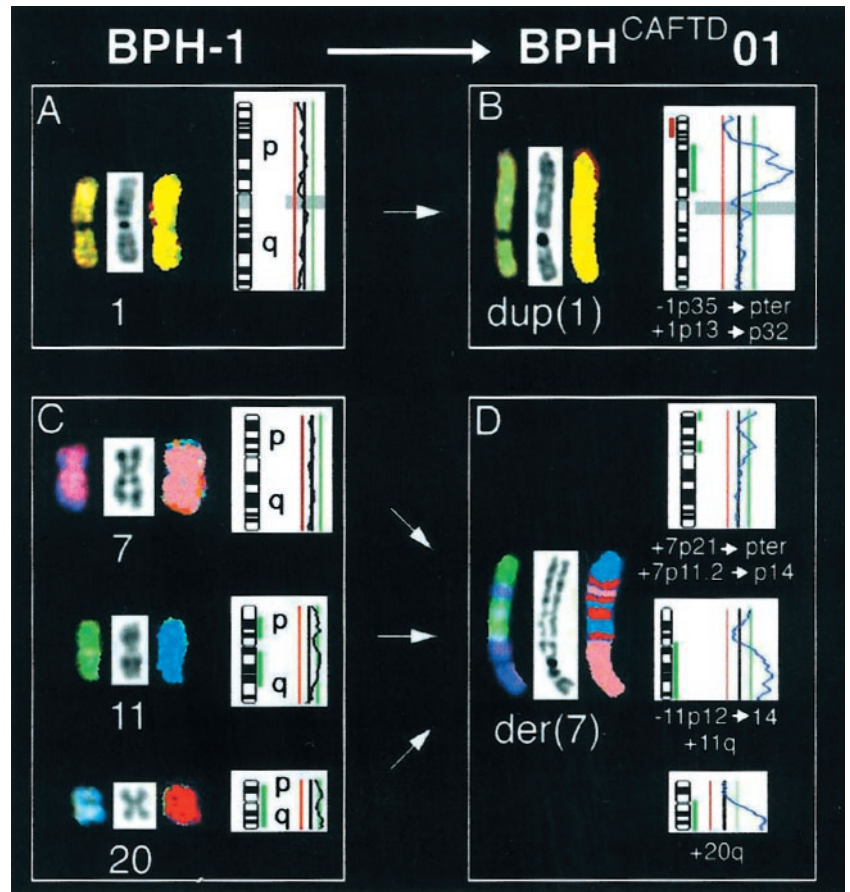[a] Color karyogram for all of the cell lines can be found at www.ncbi.nlm.nih.gov/sky/skyweb.cgi.

Fig. 2. Example of chromosomal rearrangements during tumorigenesis of BPH-1 to BPH[CAFTD]-01. *A*, normal chromosome 1 in BPH-1. *From left to right*, the display image of the hybridization, the 4′-6′-diamidino-2′phenylindole (DAPI)-stain, the spectral classification image, and the CGH profile. *Thin red line*, the threshold for a loss; *thin green line*, the threshold for a gain. *B*, duplicated chromosome 1p in BPH[CAFTD]-01. CGH now shows gain of 1p13->1p33 and loss from 1p34->1pter during tumorigenesis (*arrow*). *C*, representative chromosomes 7, 11, and 20 from BPH-1. The CGH profile of chromosome 7 is normal, whereas profiles for chromosomes 11 and 20 show gains (*thick green bars next to ideogram*). *D*, harlequin chromosome (HC) in BPH[CAFTD]-01 by SKY (*left*). CGH profiles show that formation of HC during tumorigenesis (*arrows*) results in gains of regions of 7p, 11q, and *20q* (indicated in figure).

tained in the second-generation tumors except for losses on chromosome 5, 16q, 18, and 19.

The BPH1[TETD] cell lines had a very similar CGH profile compared with the first generation CAF-derived lines, including high-level amplification of 11q. However, the BPH1[TETD] lines had high-level gain of chromosomal arm 7p and pronounced losses of 5q, 17p, and Xq. In addition, the 6p gain seen in CAF tumors was not present in the hormone-derived tumorigenic cell lines.

Microarray Analysis of BPH-1 *versus* BPH1[CAFTD]-01. To establish a gene expression profile of tumorigenic conversion and to analyze the consequences of acquired chromosomal aneuploidies on gene expression profiles, we performed microarray analysis with total RNA extracted from BPH-1, and the tumor line, BPH1[CAFTD]-01 (CAF-derived, first generation). This analysis was repeated four times. Of the 6500 cDNA targets on the NCI Oncochip,[3] ratios for 5276 named genes and hypothetical proteins (1537 of which were in

Fig. 3. BPH-1 to BPH[CAFTD]-01 tumorigenesis, correlation of genomic DNA changes with changes on cDNA microarray. Down-regulated genes (*red dots*) and up-regulated genes (*green dots*) from microarray experiments appear at their known map location. Relative DNA loss (*thick red bar next to ideogram*) and gains (*thick green bar next to ideogram*). For clarity, only genes from criteria numbers 1 and 2 in Tables 2A and 2B are displayed. For example, as shown in the key, net gain of 20q in tumor correlates with the up-regulation of two genes (*MMP-9* and *PROCR*) of the 60 genes represented on the NCI Oncochip that map to 20q (*two green dots on 20q*). ∗ (*within the known region*), genes without precise banding (*e.g., CBX-1,* 17q12–21).
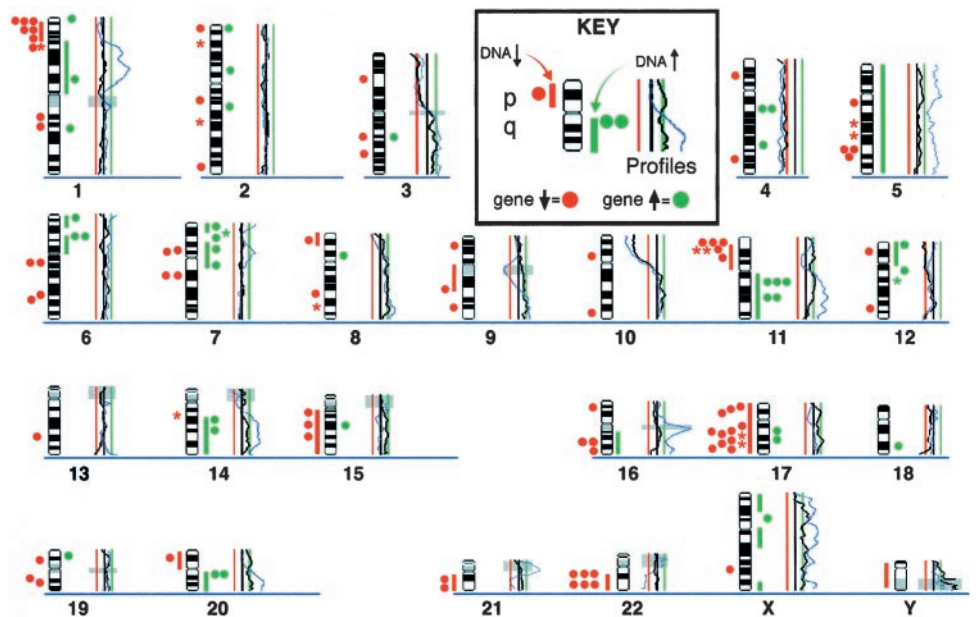
Table 2 *Correlation of genes down (A) and up (B) with changes of copy number as assessed by CGH and correlation of all mapped genes (c) down (⇓) and up (⇑) with change in DNA*

Gene selection criteria are outlined in "Materials and Methods."

	DNA change per CGH				
	⇓[a]	⇔	⇑	?	Total
A. Down groups					
Criteria					
≤0.50	12	11	5	1	29
>0.50–≤0.75 (in 5/5 arrays)	21	24	6	5	56
>0.50–≤0.75 (in 4/5 arrays)	21	17	7	0	45
	54	52	18	6	130
B. Up groups					
Criteria					
≥2.0	2	5	6	0	11
≥1.7–<2.0	1	11	11	1	23
≥1.5–<1.7	4	13	22	1	36
	7	19	39	2	77
C. Combined data					
Genes ⇓	54	52	18		
Genes ⇑	7	19	39	$P < 0.0001^b$	

[a] ⇓, DNA loss; ⇑, DNA gain; ⇔, DNA neutral; ?, genes with imprecise mapping.
[b] Value of $2 \times 3\ \chi^2$.

duplicate-or-more spots), 674 unique ESTs/cDNAs/mRNAs, and 69 "unknowns" were evaluable in ≥3 array pairs.

A total of 883 targets represented genes with coarse or no chromosomal assignment. Of this group, 34 reached threshold conditions in all 5 of the array pairs and BLAST searching revealed chromosomal band assignment for 30 of these genes. Two transcripts were increased ≥2.0-fold in all arrays: LOC56912 (ratio, 2.63) and *KDELR2* (ratio, 2.00), which we BLAST-mapped to 11q22 and 7p15–22, respectively. Conversely, 21 genes (~2.0%) were decreased <0.75 in all 5 of the array pairs including IFN-induced protein (*ISG15*: ratio, 0.20; 1p36), integrin α_3 (*ITGA3*: ratio, 0.70; 17q21), and sorting nexin 14 (*SNX14*: ratio, 0.62; ~6q13), which targets the EGF receptor for degradation.[8]

For the purpose of correlating gene expression levels with genomic copy number changes, we considered the 2856 unique genes for which chromosomal mapping positions were available. Of these, 77 (2.6%) and 130 (4.5%) genes met our criteria for expression at higher or lower levels, respectively, when compared with BPH-1 (Table 2). We were particularly interested in how chromosomal aneuploidies affected the gene expression profiles. We have, therefore, compared the expression levels of all genes (including the ones for which we have retrieved band assignment by a BLAST search) that mapped to regions of genomic copy number changes after conversion to tumorigenicity. These comparisons are summarized in Table 2 and displayed in Fig. 3. Fifty-one % of up-regulated genes mapped to regions of DNA gain, and 42% of down-regulated genes mapped to DNA loss. Areas of gene up-regulation appeared to cluster within regions of DNA gain at 1p, 7p, 11q, and 12p, and clusters of gene down-regulation occurred with regions of DNA loss at 1pter, 11p, 21, 22, and, most predominantly, chromosome 17. Interestingly, 18 (14%) of 130 down-regulated genes occurred in regions of DNA gain (predominantly 5q) but only 7 (9%) of 77 up-regulated genes occurred in regions of DNA loss. The remainder of the genes that revealed expression changes (of which approximately equal proportions result in either increased or decreased expression levels) mapped to chromosomal regions unaffected by gain or loss. The proportions of genes

[8] The complete list with expression ratios and map location can be retrieved from www.riedlab.nci.nih.gov/Publications/publications.html.

in each group were similar for three different threshold criteria (Tables 2, A and B). The association of down-regulated genes, with regions of DNA loss, and up-regulated genes, with regions of DNA gain, was statistically significant ($P < 0.0001$; Table 2C).

To address the question whether chromosomal aneuploidies uniformly affect the expression levels of genes located on these chromosomes, we compared the mean ratios for target values from all five array pairs for a particular chromosome or chromosomal arm with those of another chromosome. For this purpose, we included genes without a precise band assignment but with assignment to a chromosome arm or chromosome (*e.g.,* assignment to any region of chromosome 5 as it underwent a whole copy number gain). This increased the gene number for analysis by more than 600. Chromosome 2 was used as an internal standard because it underwent no discernible change in DNA copy number by CGH during tumorigenic conversion. In cases in which a large discrepancy existed between target number on the arrays (*e.g.,* chromosome 2 *versus* 20q), equal numbers of target values were compared, which were randomly chosen from each chromosome number set. Results showed that there was no difference in average target value when comparing chromosomes or chromosomal regions that had no change in DNA copy number during transformation of BPH-1 (*e.g.,* chromosome 2 *versus* chromosome 4 or chromosomal arm 7q; Table 3). In contrast, the values for chromosomes 11q and 20q, which are gained in copy number, were, on average, greater than for chromosome 2. Accordingly, the values for chromosome 17 and 22, which show relative loss, were, on average, lower than for chromosome 2. However, the expression levels for targets on chromosomes 5 and 14, which had a gain in copy number, were, on average, no greater than chromosome 2 ($P > 0.10$).

The two most significantly increased genomic copy number changes in the tumorigenic lines were mapped to chromosome bands 11q13→22 and 20q13→qter. Genes that were significantly up-regulated on the 11q amplicon included *cyclin D1* (ratio, 1.70; band, 11q13), c-*fos*-like antigen-1 (ratio, 1.78; band, 11q13), and the inhibitors of apoptosis (*IAP*) *1* and *2* (ratios, 2.1 and 1.75, respectively; band, 11q22). Of the 60 genes represented on the cDNA array that mapped to the 20q region, only one, *MMP-9* (ratio, 2.03; band, 20q11.2), appeared up-regulated by more than 2-fold. Two other genes, *RPS 21* and *PROCR*, reached ratios of 1.50 and 1.85, respectively. By zymography, which measures functional protein, we confirmed that MMP-9 levels were significantly elevated in the tumor line and undetectable in BPH-1. MMP-2 activity levels were used as an internal control (Fig. 4; Ref. 18). MMP-2 (which maps to 16q) expression was unchanged on microarray analysis.

We next categorized the 207 genes that changed during tumorigenic conversion of BPH-1 according to known or assumed function using databases available at http://ncbi.nlm.nih.gov. We found that a significant number of genes had putative or known roles in prostate and/or epithelial carcinogenesis, 22 of which are displayed in Table 4. These

Table 3 *Chromosome 2 target values compared with lost, neutral, and gained chromosomes*

On average, chromosome 2 values were significantly higher than for the lost chromosomes 17 and 22, no different from the neutral chromosome 4 and chromosomal arm 7q, and lower than gained chromosomal arms (*e.g.,* 11q and 20q).[a] However, chromosome 2 values were, on average, no different from chromosomes 5 and 14, which were gained in copy number. Not shown is that chromosome 5 values were, on average, higher than chromosome 22, which was lost ($P = .035$).

Loss on CGH	Neutral on CGH	Gain on CGH
Chromosome 22	Chromosome arm 7q	Chromosome 11q
$P < 0.01$	$P = 0.57$	$P = 0.02$
Chromosome 17	Chromosome 4	Chromosome arm 20q
$P < 0.001$	$P = 0.40$	$P < 0.001$

[a] Two-tailed U test, www.statibot.com.

include gains of the oncogenes *Gro1* and *2*, the hevin-like protein *SPARCL1*, *IAP*s 1 and 2, and *MMP-9*, and loss of *BRCA1*, *TC21*, *caveolin 2*, *integrin-α₃*, and *α-catenin*, among others. Such genes could be functionally assigned to three categories, which include those that favor invasion, antiapoptosis, and growth (*e.g.,* loss of tumor suppressor genes, up-regulation of oncogenes). The observed expression level changes are compatible with a phenotype shift from immortalization to tumorigenesis in a prostate cancer model. However, the majority of genes had no described role in carcinogenesis and included 55 fat/protein/carbohydrate metabolism-related genes, 23 structural/membrane proteins, 27 hematopoetic/cytokine genes, 6 IFN-related genes, and 49 others, including 7 genes that changed in a way that was counterintuitive for a prostate cancer model (see www.riedlab.nci.nih.gov/Publications/publications.html). For example, we measured a consistent up-regulation of *TIMP1*, the tissue inhibitor of the pro-invasive MMP-1. As an internal control, we correlated cDNA array data with immunohistochemistry (IHC) for vimentin [see accompanying article by Hayward *et al.* (12)]. IHC showed no vimentin expression in BPH-1 and only weak expression in BPH^CATD^-01 (12). Accordingly, vimentin expression on the arrays was weakly up-regulated (ratio, 1.40) but below our cutoff threshold for 'up-regulation.'

DISCUSSION

Epithelia-mesenchymal interactions are now thought to play a sentinel role in the initiation and progression of prostate cancer (9–11). A novel series of tissue recombination experiments revealed that prostate CAFs cause a transforming event in a large T-antigen immortalized, but nontumorigenic, prostate epithelial cell line, BPH-1 (9). Cells derived from the resulting tumors are termed BPH^CAFTD^ and remain tumorigenic even after removal of the CAF influence.

Fig. 4. Totiomic evaluation (*i.e.,* how chromosomal aberrations correlate with functional sequellae) of chromosome 20 during tumorigenesis of BPH-1. *A*, structural aberration. SKY reveals a translocation involving 22q (*yellow display image*, *pink classification color*) and 20q (*pale blue display image*, *red classification color*) in BPH^CAFTD^-01. *B*, changes on the DNA/RNA level. Merging the *black* CGH profile of BPH-1 with the *blue* profile of BPH^CAFTD^ 01 reveals that tumor has relative decrease in copy number of 20p and increase of 20q compared with BPH-1. These changes correspond to loss of a 20p gene (*JAG1*) and gain of two 20q genes (*MMP-9* and *PROCR*) on cDNA microarray analysis. *C*, microarray analysis. Expression profiling using cDNA microarrays, here represented by 1 of the 16 grids from a 6.5K NCI Oncochip used in the described experiments. *D*, changes in protein level. Finally, increased *MMP-9* gene expression as assessed by the arrays is validated on the protein level using a zymographic assay of enzymes electrophoretically separated under nonreducing conditions (18). Shown is evidence that MMP-2 activity (*lower white bands*) is similar in BPH-1 and BPH^CAFTD^-01 but that MMP-9 activity is higher in BPH^CAFTD^-01 (*upper white band*).

Table 4 *Genes identified as down- or up-regulated from microarray analysis of BPH-1 to CAFTD 01 tumorigenesis, grouped by known or putative function*

Shown are Unigene abbreviation, known or BLAST-mapped locus, mean ratio on microarray pairs, and change of DNA copy number (δDNA) at this region, as assessed by CGH (gain = ⇑, loss = ⇓, neutral = ⇔). A "?" indicates imprecise mapping despite Human Genome BLAST with GenBank sequence.

Gene	Map	Ratio	δDNA
Proinvasion			
CSTA	3q21	0.37	⇔
KRT 19	17q21	0.48	⇓
CTNNA	5q31	0.56	⇑
ITGA3	17q21-22	0.70	⇓
SPARCL1	?7pter	1.52	?
MMP-9	20q11.2	2.03	⇑
KRT 7	12q12-21	1.96	⇔
CTSW	11q13	1.80	⇑
Prosurvival			
TRAIL	3q26	0.54	⇔
CALM3	19q13.2	0.62	⇔
CDC 42	1p36.1	0.67	⇓
SARP2	8p12	2.56	⇔
RAC1	7p22	2.10	⇑
IAP1,2	11q22	2.1, 1.75	⇑
Progrowth			
Tumor suppressor genes			
TC21	11p13-pter	0.47	?
TSG101	11p15	0.73	⇔
SNX14	6q13	0.62	⇔
BRCA1	17q21	0.72	⇓
Oncogenes			
GRO1,2	4q21	2.9, 2.6	⇔
RAB3A	19p13.2	1.93	⇔
cFOS-L-1	11q13	1.78	⇑
PIM-1	6p21.2	1.54	⇑

Similarly, BPH-1 forms tumors after recombination with embryonic rUGM when the host mice are treated with TE, thus producing BPH^TETD^ lines (12). Removal of the TE influence does not reverse tumorigenicity, as described in the accompanying article by Hayward *et al.* (12). This suggests that acquired genetic aberrations could provide the means to establish CAF- and hormone-independence. It would, therefore, be intriguing to identify the genetic changes that correlate with and contribute to the maintenance of this phenotypic conversion.

The application of molecular cytogenetics, and in particular, CGH, to the detection of chromosomal imbalances during tumorigenesis has provided sound evidence that specific chromosomal aberrations accompany or cause the stepwise progression from normal epithelium to dysplastic lesions and, eventually, invasive carcinomas (19). We, therefore, chose to follow the sequence of chromosomal aberrations in these model systems of prostate cancer using SKY, CGH, and fluorescent *in situ* hybridization. Using the same cell lines, changes in the gene expression profiles were monitored using cDNA array technology. This allowed us not only to identify which genes are subject to increased or decreased expression during immortalization and tumorigenic conversion, but also to query the consequences of chromosomal aneuploidy with respect to gene expression levels. Hypothetically, chromosomal aneuploidies could have three possible consequences: (*a*) the expression of all or most genes located on a chromosome is affected by chromosomal gain or loss; (*b*) the expression of only a few genes, the reduced or increased expression of which is critical for tumorigenesis, is the target of chromosomal aneuploidy during tumorigenesis. Thus, whole chromosome copy number changes may simply reflect an economical and readily achievable mechanism for the cell to acquire and maintain such expression changes. This would implicate silencing mechanisms for all other genes located on chromosomes present in increased copy numbers; or (*c*) chromosomal aneuploidies do not affect gene expression levels.

Karyotypic analysis of BPH-1 by SKY and CGH reveals a plethora of chromosomal aberrations and resulting genomic imbalances. Of
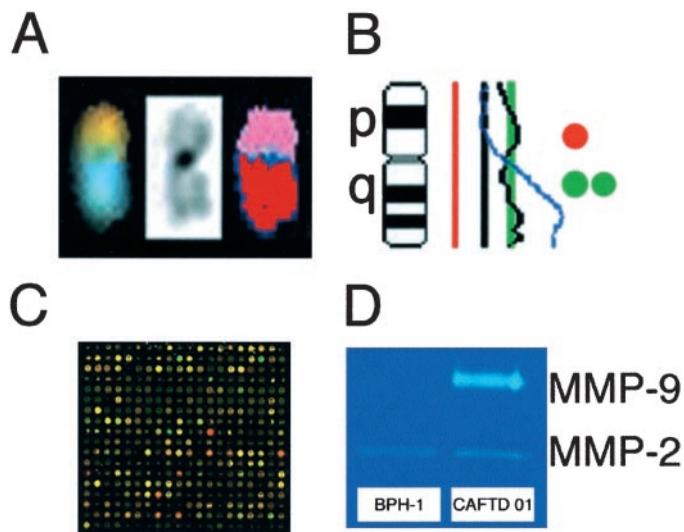
note, as BPH-1 undergoes tumorigenesis during recombination with CAF, specific and complex additional chromosomal aberrations occur that lead to recurring copy number changes. CGH showed that during tumorigenic conversion, regardless of the exact karyotypic mechanism, all of the tumors had high-level amplification of chromosome bands 11q13→q22 and chromosome arm 20q. All of the tumors had gains of 1p13→p33 and loss of 1p34→pter (because of an interstitial duplication) and loss of 11p, as seen in advanced prostate cancers (1, 2, 7). Coincident with the development of CAF-independent lines from first generation BPH[CAFTD]s, we detected the loss of chromosomes 5, 16q, 17, 19, and more pronounced copy number reduction of 20p. Loss of 16q has been previously shown to correlate with decreased expression of E-cadherin in an HPV-transformed prostate line (20).

To assess the consequence of the above genomic imbalances on the gene expression levels during BPH-1 tumorigenesis, we used cDNA microarrays. The results were subject to two considerations. Firstly, we were interested in how chromosomal copy number changes influence RNA and levels, and secondly, whether we can detect any functional relationships among genes or gene clusters that were subject to either increased or repressed expression. About 3% of the mapped genes on a 6.5K array changed significantly during tumorigenesis of BPH-1, a percentage similar to that reported in microarray analyses of the malignant progression of lymphomas, the quiescent fibroblast response to serum, and the T-cell response to calcium (21–23).

Fifty-one % of up-regulated and 41% of down-regulated genes mapped to regions of corresponding DNA gain and loss, respectively. However, ~14% of down-regulated genes appeared with regions of DNA gain, namely genes at 5q; and 9% of up-regulated genes appeared in regions of DNA loss. The remainder of altered genes mapped to regions that were unchanged in DNA copy number during tumorigenic conversion of BPH-1. For example, the oncogene *GRO-1* was up-regulated 2.7-fold in all five of the array pairs yet mapped to a region that is neutral during tumorigenesis in terms of genomic copy number change (4q21). Therefore, about 50% of significant gene expression changes, as assessed on our level of stringency for cDNA microarrays, do not appear on regions of corresponding changes in DNA copy number. However, Table 2C convincingly suggests ($P < 0.0001$) that average gene expression levels are related to DNA gain and loss.

In cases in which an entire chromosomal arm was gained, only a few genes, and in some instances only one gene, were overexpressed. For example, on chromosome 20q, which is present in 3–7 copies in the tumorigenic cell lines, only one gene, *MMP-9*, showed more than a 2-fold increase in expression levels. This elevation of gene message correlated with marked increases in functional MMP-9 product, as detected by a zymographic assay (Fig. 4; Ref. 18). These observations suggest that DNA copy number may influence, but does not override, transcriptional control mechanisms that are already in place. It also appears that there is a correlation of relative chromosome copy number and the average global expression levels of all of the genes on the chromosome or chromosomal arm. For example, for the 121 gene targets mapped to chromosome 11q (which was gained in copy number), the average target ratio value was greater than the average ratio value for the 215 targets mapped to chromosome 2 (which was neutral in copy number). However, only 9 (7%) of the "11q genes" reached threshold values for "upregulation." We cannot deduce from our analyses to what extent the increase in the average transcription level of all of the genes on chromosome arms 11q and 20q, rather than the significant, high-level increase of a few genes, provide the immortalized cells with the transcriptome required for tumorigenic conversion. What is clear, however, is that a gain or loss of chromosomes

and chromosomal subregions does not directly translate to, respectively, increased or decreased expression level changes in the same ratio identified for genomic imbalances.

From a gene-function point of view, we found that genes the expression of which changes during BPH-1 tumorigenesis appear to cluster within gene families that ultimately favor invasion, cell survival, and enhanced growth. However, the overall pattern of gene expression changes that have been observed fits well in a prostate tumor model. Many of these genes have been previously implicated in prostate tumorigenesis. For example, invasiveness may be favored with the observed alterations in extracellular matrix turnover (⇑*MMP-9*), decreased basement membrane stability (⇓ α integrins) and decreased functional E-cadherin complex (⇓ α-catenin). Cell survival may result from alterations disfavoring caspase- (⇑ *IAPs*, ⇓ *TRAIL*), β-catenin- (⇑ *SARP2*), and/or Bcl-2-mediated (⇑ cyclin D1) apoptosis or other downstream apoptotic events (⇑ RAC1). Favorable growth parameters may be influenced by decreased tumor suppressor genes (⇓ *BRCA1*, *TSG 101*, and *TC21*) and and/or up-regulated oncogenes (⇑ *GRO1* and *GRO2, PIM-1,* and the *Ras*-like oncogene, *RAB3A*).

In conclusion, tumorigenesis of BPH-1 involves complex chromosomal rearrangements that result in genomic imbalances. These, in turn, correlate with significant expression changes of a small fraction of genes that ultimately appear to favor a highly malignant and invasive phenotype. However, an absolute correlation between genomic copy number and gene expression levels was not observed, nor would it have been expected, because 50% of the genes with modified expression levels map to regions unaffected by genomic imbalances. The correlation of SKY and CGH results with gene expression levels measured using cDNA microarrays has allowed us to identify how chromosomal aberrations, and in particular those that result in genomic copy number changes, affect gene expression profiles. This and similar studies will provide important baselines for understanding the complex networks of genetic pathways in the frame of the invariably observed aneuploidy in cancer cells. The fact that only a few target genes seem to be subject to significant changes in expression levels induced by chromosomal aneuploidies suggests that the combined analyses of genomic imbalances and gene expression profiles could expedite the identification and molecular cloning of cancer-associated genes.

ACKNOWLEDGMENTS

APPENDIX

International System for Human Cytogenetics Nomenclature (ISCN) Karyotypes Tables

ISCN Karyotypes of BPH-1, CAFTDs, and TETDs as assessed by SKY. Underlined markers in BPH-1 are those that recur unchanged in all TD lines.

I. Parental Line

BPH-1
60–73, XY, +X, +Y, +1, +2, i(3)(q10) **[M1]**, −4, +5, i(5)(p10) **[M2]**, +6, +7, der(8)t(8;9)(p21;q13) **[M3]**, der(8;12)(p11.2;p12) **[M4]**, der(8)t(8; 17)(p11.2;q11.2) **[M5]**, +9, der(9;12)t(9;12)(p10;p10) **[M6]**, der(10)t(10; 12)(p11.2;HSR) **[M7]**, der(10)t(10;12)(p11.2;q13) **[M8]**, der(10)t(10; 15)(q10;q10)del(15)(q21) **[M9]**, de(10)t(16HSR::12HSR::16HR::12HSR:: 10p11.2→10qter)**[M10],** der(10)t(14;12;10)(14qter→14q22::12q24.1→ 12q12::10p11.2→10qter) **[M11]**, dic(10;10)t(10;12;12;10)(10qter→

10p11.2::12?::12?::10p11.2→10qter) **[M12]**, +11, dic(11;12)t(11;12)(q25; q13) **[M13]**, −12, +13, +14, +15, der(16)t(9;16)(q21;p11.2) **[M14]**, +17, +20, +21, +22 [cp15].

II. CAFTD Lines

1. BPH^{CAFTD}-01 (first generation derived from BPH-1)

50–64 XY, +X, **[M1]**, **[M3]**, **[M8]**, **[M14]**, dup (1)(p23→p36) **[M15]**, +2, +3, der(3)t(3;12)(p21;p12) **[M16]**, +5, +6, tic(7;11;20)t(11;20;7;20;11;20; 11;20;7)(11p11.2→q13::20q?::7?::20?cen::11?::20q?::11p12→q14::20?::7p22→ qter) **[M17]**, der(8)t(8;14)(p11.2;q12?3) **[M18]**, der(11)t(17;11;20;9)(17q25→ 17q22::11p15→11q13::20?::9q22→9q34) **[M19]**, +14, −15, der(15)t(9; 15)(q2?;q24) **[M20]**, der(10;16)t(10;16)(10q24→10q11.2::16p11.2→16qter)del (10)(q24) **[M21]**, −17, +18, +20, der(22)t(11;7;20;11;22)(11p15→11q13:: 7HSR::20q?::11q?::22p11.2→22qter) **[M22]** [cp8].

2. BPH^{CAFTD}-2 (second generation derived from CAFTD-01 without CAF)

58–65 XY, +X, +Y, **[M1]**, **[M3]**, **[M8]**, **[M16]**, **[M18]**, **[M20]**, **[M21]**, +2, +3, +5, +6, der(7)t(13;20;7)(q2? →q3?::20q?::7p22→qter) **[M23]**, der(8)t(13; 22;8)(13qter→q2?::22q13::8p12→qter) **[M24]**, −16, der(17)t(22;20;11;17) (22q1?::20q12?3::11q13::17p11.2→qter) **[M25]**, der(20)t(22;11;22;20;7;22) (22q13::q1?3→q2?::q13::7p2?1::22p11.2→22qter) **[M26]**, +21, −22, der(22)t (13;7;20;11;22)(13qter→q31::7?::20q?::11q1?3→2?::22p11.2→qter) **[M27]** [cp10].

3. BPH^{CAFTD}-03 (first generation derived from BPH-1)

63–72 XY, +X, +Y, **[M1]**, **[M3]**, **[M8]**, **[M18]**, **[M20]**, **[M21]**, +2, +3, del (3)(p10) **[M28]**, +5, +6, trc (7;11)t(8;20;7;20;11;20;7)(8qter→q21.2::20q? →20cen::7?p::20q?::11q23→11p15::20q?::7p15→7qter) **[M29]**, trc (7;11;20)t (9;20;11;7;20;11;20;7)(9q34→9q22::11p?::20q13.1→20p11.2::11q1?3→11q1?4:: 7p?::20q?::11p15→11q23::7p21.3→7qter) **[M30]**, −8, −9, −10, dic (11; 13)(q23;p11.2) **[M31]**, −12, der(16)t(16;17)(p13;p12) **[M32]**, der(22)t(13;11;20; 22)(13qter→13q3?::11q?::20q::22p11.2→22qter) **[M33]** [cp7].

4. BPH^{CAFTD}-04 (second generation derived from CAFTD 03)

54–65 XY, +X, +Y, **[M1]**, **[M3]**, **[M8]**, **[M20]**, **[M21]**, +2, +3, +5, +6, dic(7;11)t(13;20;11;7;20;11;20;7)(13qter→13q2?2::20?::11q1?::7p?::20?::11q13→ 11p11.2::7p13→7qter) **[M34]**, dic(11;22)t(9;11;22)(9qter→9q22::11p11.2→ 11q13::20?::11?::22p11.2→22qter) **[m35]**, −16, +17, +18, +19, +20, +21, der(22)t(11;20;22)(11q1?3→11q2?2::20q?::22p11.2→22qter) **[M36]** [cp8].

III. TE/rUGM TD (TETD) Cell Lines

1. BPH^{TETD}-A

46–63, XY, +X, −Y, **[M1]**, **[M3]**, **[M8]**, der(X;8)t(X;8)(q11.1;q11.1) **[M37]**, t(1;3)(1pter→1p31::3p13→3qter;3pter→3p13::1p31→1qter) **[M38]**, +2, +3, −4, t(4;11)(4pter→q13::11q13→11qter;11pter→11q13::4q13→4qter) **[M39]**, der(4)t(4;11;18)(4pter→4q13::11q13→q2?::18?) **[M40]**, der(5)t(5;11;20;11;3) (5pter→5q11.2::11?::20q12→20q13.2::11q12→11q14::3q28→3qter) **[M41]**, −7, der(7)t(22;11;20;7)(9?::11q12→11q14::9?::7p21→7qter) **[M42]**, −8, t(8;14) (8pter→8p11.2::14p11.1→14q13;14qter→14q13::8p11.2→8qter) **[M43]**, −10, t(10;12)(p10;q10) **[M44]**, −11, der(11;17)(17qter→17p11.1::11q13→11p11.1:: 20q?::9q31→9qter) **[M45]**, −15, der(15)t(15;22)(q 25;q?) **[M46]**, −18, −19, der(19)t(19;7?)(q13.1;p?) **[47]**, der(19)t(19;7;21)(q13.1;p?;q22) **[M48]**, −21, −22 [cp8].

2. BPH^{TETD}-B

47–62 XY, −Y, **[M1]**, **[M3]**, **[M8]**, **[M15]**, **[M18]**, **[M20]**, **[M21]**, **[M37]**, **[M39]**, **[M40]**, **[M45]**, **[M47]**, **[M48]**, −1, der(3)t(1;3)(1pter→1p31::3p13→ 3qter)**[M49]**, −4, +6, −8, −9, −10, −11, der(15)t(14;15)(q2?4;q24)**[M50]**, +16, der(17)t(?;17;?;?)(?;p11.2→q22;?;?) **[M51]**, +20, −21, −22, der(22)t(19; 22)(q13.1;22cen) **[M52]** [cp10].

REFERENCES

1. Nupponen, N. N., Hyytinen, E. R., Kallioniemi, A. H., and Visakorpi, T. Genetic alterations in prostate cancer cell lines detected by comparative genomic hybridization. Cancer Genet. Cytogenet., *101:* 53–57, 1998.

2. Nupponen, N. N., and Visakorpi, T. Molecular cytogenetics of prostate cancer. Microsc. Res. Tech., *51:* 456–463, 2000.

3. Jenkins, R. B., Qian, J., Lee, H. K., Huang, H., Hirasawa, K., Bostwick, D. G., Proffitt, J., Wilber, K., Lieber, M. M., Liu, W., and Smith, D. I. A molecular cytogenetic analysis of 7q31 in prostate cancer. Cancer Res., *58:* 759–766, 1998.

4. Ruijter, E. T., Miller, G. J., van de Kaa, C. A., van Bokhoven, A., Bussemakers, M. J., Debruyne, F. M., Ruiter, D. J., and Schalken, J. A. Molecular analysis of multifocal prostate cancer lesions. J. Pathol., *188:* 271–277, 1999.

5. Zitzelsberger, H., Kulka, U., Lehmann, L., Walch, A., Smida, J., Aubele, M., Lorch, T., Hofler, H., Bauchinger, M., and Werner, M. Genetic heterogeneity in a prostatic carcinoma and associated prostatic intraepithelial neoplasia as demonstrated by combined use of laser- microdissection, degenerate oligonucleotide primed PCR and comparative genomic hybridization. Virchows Arch., *433:* 297–304, 1998.

6. Kallioniemi, O. P., and Visakorpi, T. Genetic basis and clonal evolution of human prostate cancer. Adv. Cancer Res., *68:* 225–255, 1996.

7. Forsslund, G., and Zetterberg, A. Ploidy level determinations in high-grade and low-grade malignant variants of prostatic carcinoma. Cancer Res., *50:* 4281–4285, 1990.

8. Forsslund, G., Esposti, P. L., Nilsson, B., and Zetterberg, A. The prognostic significance of nuclear DNA content in prostatic carcinoma. Cancer (Phila.)., *69:* 1432–1439, 1992.

9. Hayward, S. W., Dahiya, R., Cunha, G. R., Bartek, J., Deshpande, N., and Narayan, P. Establishment and characterization of an immortalized but non-transformed human prostate epithelial cell line: BPH-1. In Vitro Cell Dev. Biol. Anim., *31:* 14–24, 1995.

10. Olumi, A. F., Grossfeld, G. D., Hayward, S. W., Carroll, P. R., Tlsty, T. D., and Cunha, G. R. Carcinoma-associated fibroblasts direct tumor progression of initiated human prostatic epithelium. Cancer Res., *59:* 5002–5011, 1999.

11. Wang, Y., Sudilovsky, D., Zhang, B., Haughney, P. C., Rosen, M. A., Wu, D. S., Cunha, T. J., Dahiya, R., Cunha, G. R., Hayward, S. W. A human prostatic epithelial model of hormonal carcinogenesis. Cancer Res., *61:* 6064–6072, 2001.

12. Hayward, S. W., Wang, Y., Cao, M., Hom, Y. K., Zhang, B., Grossfeld, G. D., Sudilovksy, D., Cunha, G. R. Malignant transformation in a nontumorigenic human prostatic epithelial cell line. Cancer Res., *61:* in press, 2001.

13. Veldman, T., Vignon, C., Schrock, E., Rowley, J. D., and Ried, T. Hidden chromosome abnormalities in haematological malignancies detected by multicolour spectral karyotyping. Nat. Genet., *15:* 406–410, 1997.

14. Schrock, E., du Manoir, S., Veldman, T., Schoell, B., Wienberg, J., Ferguson-Smith, M. A., Ning, Y., Ledbetter, D. H., Bar-Am, I., Soenksen, D., Garini, Y., and Ried, T. Multicolor spectral karyotyping of human chromosomes. Science (Wash. DC), *273:* 494–497, 1996.

15. Ghadimi, B. M., Schrock, E., Walker, R. L., Wangsa, D., Jauho, A., Meltzer, P. S., and Ried, T. Specific chromosomal aberrations and amplification of the AIB1 nuclear receptor coactivator gene in pancreatic carcinomas. Am. J. Pathol., *154:* 525–536, 1999.

16. Ross, D. T., Scherf, U., Eisen, M. B., Perou, C. M., Rees, C., Spellman, P., Iyer, V., Jeffrey, S. S., Van de Rijn, M., Waltham, M., Pergamenschikov, A., Lee, J. C., Lashkari, D., Shalon, D., Myers, T. G., Weinstein, J. N., Botstein, D., and Brown, P. O. Systematic variation in gene expression patterns in human cancer cell lines. Nat. Genet., *24:* 227–235, 2000.

17. Alizadeh, A. A., Eisen, M. B., Davis, R. E., Ma, C., Lossos, I. S., Rosenwald, A., Boldrick, J. C., Sabet, H., Tran, T., Yu, X., Powell, J. I., Yang, L., Marti, G. E., Moore, T., Hudson, J., Jr., Lu, L., Lewis, D. B., Tibshirani, R., Sherlock, G., Chan, W. C., Greiner, T. C., Weisenburger, D. D., Armitage, J. O., Warnke, R., Staudt, L. M., *et al.* Distinct types of diffuse large B-cell lymphoma identified by gene expression profiling. Nature (Lond.), *403:* 503–511, 2000.

18. Oliver, G. W., Leferson, J. D., Stetler-Stevenson, W. G., and Kleiner, D. E. Quantitative reverse zymography: analysis of picogram amounts of metalloproteinase inhibitors using gelatinase A and B reverse zymograms. Anal. Biochem., *244:* 161–166, 1997.

19. Ried, T. Heselmeyer-Haddad, K., Blegen, H., Schroeck, E., Auer, G. Genomic changes defining the genesis, progression, and malignancy potential in solid human tumors: a phenotype/genotype correlation. Genes Chromosomes Cancer, *25:* 195–204, 1999.

20. Chin, R. K., Hawkins, A. L., Isaacs, W. B., and Griffin, C. A. E1A transformed normal human prostate epithelial cells contain a 16q deletion. Cancer Genet. Cytogenet., *103:* 155–163, 1998.

21. Li, S., Ross, D. T., Kadin, M. E., Brown, P. O., and Wasik, M. A. Comparative genome-scale analysis of gene expression profiles in T cell lymphoma cells during malignant progression using a complementary DNA microarray. Am. J. Pathol., *158:* 1231–1237, 2001.

22. Iyer, V. R., Eisen, M. B., Ross, D. T., Schuler, G., Moore, T., Lee, J. C., Trent, J. M., Staudt, L. M., Hudson, J., Jr., Boguski, M. S., Lashkari, D., Shalon, D., Botstein, D., and Brown, P. O. The transcriptional program in the response of human fibroblasts to serum. Science (Wash. DC), *283:* 83–87, 1999.

23. Feske, S., Giltnane, J., Dolmetsch, R., Staudt, L. M., and Rao, A. Gene regulation mediated by calcium signals in T lymphocytes. Nat. Immunol., *2:* 316–324, 2001.